WILEY | Hindawi

Retraction

Retracted: Helicid Improves Lipopolysaccharide-Induced Apoptosis of C6 Cells by Regulating SH2D5 DNA Methylation via the CytC/Caspase9/Caspase3 Signaling Pathway

Contrast Media & Molecular Imaging

This article has been retracted by Hindawi following an investigation undertaken by the publisher [1]. This investigation has uncovered evidence of one or more of the following indicators of systematic manipulation of the publication process:

(1) Discrepancies in scope
(2) Discrepancies in the description of the research reported
(3) Discrepancies between the availability of data and the research described
(4) Inappropriate citations
(5) Incoherent, meaningless and/or irrelevant content included in the article
(6) Peer-review manipulation

The presence of these indicators undermines our confidence in the integrity of the article's content and we cannot, therefore, vouch for its reliability. Please note that this notice is intended solely to alert readers that the content of this article is unreliable. We have not investigated whether authors were aware of or involved in the systematic manipulation of the publication process.

Wiley and Hindawi regrets that the usual quality checks did not identify these issues before publication and have since put additional measures in place to safeguard research integrity.

We wish to credit our own Research Integrity and Research Publishing teams and anonymous and named external researchers and research integrity experts for contributing to this investigation.

The corresponding author, as the representative of all authors, has been given the opportunity to register their agreement or disagreement to this retraction. We have kept a record of any response received.

References

[1] Y. Zhang, M. Wang, X. Zhang et al., "Helicid Improves Lipopolysaccharide-Induced Apoptosis of C6 Cells by Regulating SH2D5 DNA Methylation via the CytC/Caspase9/Caspase3 Signaling Pathway," *Contrast Media & Molecular Imaging*, vol. 2022, Article ID 9242827, 13 pages, 2022.

WILEY | Hindawi

Research Article

Helicid Improves Lipopolysaccharide-Induced Apoptosis of C6 Cells by Regulating SH2D5 DNA Methylation via the CytC/Caspase9/Caspase3 Signaling Pathway

Yuan Zhang [1,2] **Mei Wang,**[1,2] **Xiaotong Zhang,**[1,2] **Zhenyi Jiang,**[1,2] **Yuanxiang Zhang,**[2] **Xiangjun Fu,**[1,2] **Yanna Li,**[1,2] **Danping Cao,**[1,2] **Jun Han** [2,3] **and Jiucui Tong** [1,3]

[1]*The First Affiliated Hospital of Wannan Medical College, Yijishan Hospital, Wuhu 241001, Anhui, China*
[2]*Wannan Medical College, Wuhu 241002, Anhui, China*
[3]*Anhui Provincial Engineering Laboratory for Screening and Re-evaluation of Active Compounds of Herbal Medicines, Southern Anhui, Wuhu 241002, Anhui, China*

Correspondence should be addressed to Jun Han; hanjun@wnmc.edu.cn and Jiucui Tong; tongjiucui@wnmc.edu.cn

Received 26 November 2021; Revised 30 December 2021; Accepted 10 January 2022; Published 31 January 2022

Academic Editor: Yuvaraja Teekaraman

DNA methylation is reportedly associated with stress responses and depression. Treatment with antidepressants can regulate DNA methylation and, subsequently, gene expression in the hippocampus. Hence, DNA methylation is a potential target for treatment of depression. Screening of high-throughput data of a rat model of chronic unpredictable mild stress revealed relatively low expression of SH2 domain-containing 5 (SH2D5). SH2D5 can be overexpressed by treatment with helicid. Therefore, in order to further explore the role of SH2D5 in depression and whether helicid mediates the DNA methylation of SH2D5 as a potential antidepressant role, SH2D5 was overexpressed in C6 cells as a lipopolysaccharides (LPS)-induced model of depression. The expression levels of Bax, Bcl-2, Bad, and Daxx, and changes to the CytC/caspase9/caspase3 signal pathway were detected by qRT-PCR and Western blot analyses. After treatment with helicid or silencing of SH2D5, the above indices were detected. The results showed that helicid regulated the CytC/caspase9/caspase3 signaling pathway and improved the apoptosis indices of C6 cells through the overexpression of SH2D5. Interestingly, silencing of SH2D5 reversed the effects of helicid on the above indices. Then, in order to study the underlying mechanism, the cells were administered to helicid or 5-aza-2′-deoxycytidine (5-AzaD) and expression of SH2D5 was detected by qRT-PCR and Western blot analyses, while to assess the DNA methylation level of SH2D5 using bisulfite sequencing/PCR. The results showed that SH2D5 was hypermethylated with low expression in LPS-induced C6 cells, which was reversed by helicid and 5-AzaD. These results suggest that helicid may affect the CytC/caspase9/caspase3 apoptosis signaling pathway and improve the apoptosis indices by mediating DNA methylation of SH2D5.

1. Introduction

Depression is a relatively common mental disorder characterized by listlessness, guilt, low self-worth, sleep disturbances, changes in appetite, fatigue, inattention, and even suicidal thoughts. It is estimated that 350 million people worldwide suffer from depression, but less than half of them receive effective treatment. According to some surveys, the lifetime prevalence rate of depression (the proportion of patients who have suffered from depression in their lifetime) is 6.8%, and the 12-month prevalence rate (the proportion of

patients who have suffered from depression within 12 months) is 3.6% [1]. Although the specific mechanism of depression remains indistinct, various hypotheses have been put forward involving monoamine neurotransmitters and receptors, cytokines, the neuroendocrine system, neurotrophic factors, and epigenetic mechanisms, among others [2]. For now, antidepressants are mainly adopted for the treatment of depression, and selective serotonin reuptake inhibitors are mainly adopted, although 50%–60% of cases are complicated by drug resistance, mental disorders, and reproductive disorders [3]. These clinical phenomena

indicate that the occurrence and development of depression also involve other molecular mechanisms, including the inflammatory response and epigenetics, which have been the most widely studied [4].

Clinical and animal studies have confirmed associations of decreased hippocampal volume and weight and apoptosis with depression. Hippocampal injury (hippocampal volume reduction and excessive neuronal death) is considered an important marker of the pathogenesis of depression [5, 6]. Numerous studies have linked apoptosis to hippocampus damage. Mitochondria are the energy source of cells and maintain life as a multifunctional organelle. Over and above the regulation of heat and programmed cell death, mitochondria are also involved in the production of adenine phosphate [7, 8].

Neuronal apoptosis is an important pathogenic factor of depression. Neurogenesis is mainly regulated by proinflammatory cytokines, which is a dynamic process involving differentiation, proliferation, and death of neural progenitor cells/stem cells [9]. Evidence suggests that the regulation of cytokine expression and apoptosis is also involved in the efficacy of antidepressants. Changes in mitochondrial levels of Bcl-2-associated X protein (Bax), BCL2-associated agonist of cell death (Bad), caspase3, death-associated protein 6 (Daxx), and B-cell lymphoma 2 (Bcl-2) are established markers of lipopolysaccharide (LPS)-induced apoptosis [10]. The mitochondrial death pathway, also known as the endogenous cell death pathway, induces cell death in response to increased oxidative stress, serum deprivation, and DNA damage via regulation of the antiapoptosis B-cell lymphoma (Bcl)-2 protein, which inhibits the proapoptotic Bcl-2 family proteins Bax and Bad. In response to stress, the activated Bax/Bad peptide complex passes through the mitochondrial outer membrane, allowing cytochrome C, the serine protease Omi, also known as high-temperature demand protein A2, and the second mitochondria-derived activator of caspases/direct inhibitor of low phosphorus apoptosis binding protein (Smac/DIABLO) to enter the cytoplasm and activate the caspase cascade [11, 12].

Animal and human studies have shown that epigenetic mechanisms can regulate DNA transcription in response to environmental factors and may play a role in the pathological and physiological processes of depression [13]. Epigenetics refers to changes in expression level of a gene not involving changes in the DNA sequence, such as DNA methylation, histone modification, noncoding RNA, and chromatin remodeling [14]. DNA methylation means modification of the cytosine rings in a CpG dinucleotide using covalent binding of a methyl group of carbon 5 of cytosine of CpG dinucleotide in the genome by DNA methyltransferase. Abnormal DNA methylation and subsequent aberrant gene expression are reportedly related to depression [15]. In addition, the downregulation of N-myc downstream regulated gene 4 (NDRG4) is closely related to epigenetic regulation of DNA methylation, which weakens mitochondrial function and apoptosis [16]. DNA methylation is significantly increased in the cortex of depressed mice, while antidepressant treatment can reduce DNA methylation levels [17]. Moreover, DNA methylation, which

is influenced by environmental stimuli, directly regulates the expression of genes related to apoptosis, thereby providing a potential mechanism of gene-environment interactions in the pathophysiology of depression [18].

The SH2 domain-containing 5 (SH2D5) gene is coded by Chr1 120719731–20732837 and produces a protein that is expressed in the placenta and testis, and highly expressed in the brain, where it regulates many physiological processes associated with the nervous system. Low levels of the nucleotide guanosine triphosphatase Rac1 induce changes to SH2D5 expression in the hippocampus, which may lead to reductions in axons and dendrites, resulting in impaired brain development [19]. It has been reported that SH2D5 affects cell proliferation by restraining the activation of the Janus kinase 2 signal transduction and activator of transcription 3 pathways induced by interleukin 6 [20]. A previous meta-analysis found that methylation of the CpG site of SH2D5 may be involved in the regulation of synaptic plasticity, although abnormal DNA methylation may downregulate SH2D5 expression [21].

Helical (4-formylphenyl-β-D-allopyranoside) is a bioactive monomer isolated from longan fruit, which is clinically used for treating neurasthenia and migraine [22], as shown in Figure 1. Previous studies have found that helicid improves the depressive behavior of chronic unpredictable mild stress rat model, reduces the hippocampal inflammatory response to stressed rats, reduces the excessive oxidative stress and overactivation of C6 cells induced by LPS, and increases the expression of brain-derived neurotrophic factor (BDNF), which is the main neurotrophic factor of maintaining and surviving neuronal and synaptic plasticity [23–25].

It is well known that LPS can stimulate an inflammatory response in C6 cells. A C6 cell model of LPS-induced neuritis has been widely as an in vitro model of depression [26]. Based on the above research, the aim of the present study was to determine whether SH2D5 gene methylation regulates LPS-induced inflammation of C6 cells and to elucidate the regulatory function and underlying mechanism of helicid on SH2D5 gene methylation.

2. Materials and Methods

2.1. Cell Culture and Experimental Design. Rat glioma cell C6 (Cybertron Biotechnology Co., Ltd., Shanghai, China) was cultured in a medium containing 100 μg/mL streptomycin, 100 U/mL penicillin (Hyclone Laboratories, Inc), and 10% fetal bovine serum (Gibco, Carlsbad, CA, USA) in DMEM (Hyclone Laboratories, Inc., South Logan, UT, USA), and cultured in a constant temperature cell incubator (37°C, CO2 volume fraction 5%). The normal group cells were cultured in untreated complete medium. The cells in the LPS group were cultured in the medium supplemented with LPS. For cells requiring transfection, streptomycin and penicillin were not added to the medium.

In order to investigate the function and mechanism of SH2D5, C6 cells ($\sim 5 \times 10^4$) in the logarithmic growth phase were seeded into the wells of a six-well plate, incubated in a moistened incubator for 12 h to allow adhesion, and then transfected with plasmids encoding SH2D5 using
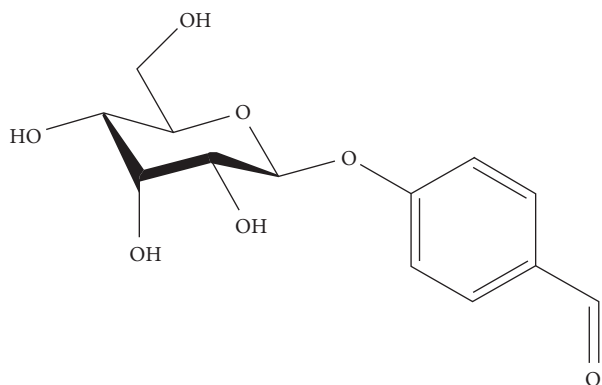
Figure 1: Structure formula of helicid. MW: 284.2 g/mol, SID: 126631785 [CID: 7573800], melting point: 199–200°C.

Lipofectamine™ 3000 Transfection Reagent (Thermo Fisher Scientific, Waltham, MA, USA) for 24 h. Subsequently, 200 μg/mL LPS (E. coil 0111: B4, Sigma-Aldrich, St. Louis, MO, USA) was added to the cells. In the back of LPS stimulation for 24 h, total RNA or total protein was extracted from the following groups of cells for subsequent analysis: control, LPS, LPS + negative control (NC), and LPS+SH2D5-overexpression.

For purpose of studying the effect and specific mechanism of helicid on SH2D5 function, C6 cells (~5×10^4) in the logarithmic growth phase were seeded into the wells of a six-well plate, placing in a wet incubator and standing for 12 h until the cells adhere to the wall, and then transfected with small interfering RNA (siRNA) with Lipofectamine™ 3000 Transfection Reagent for 6 h. Afterward, the cells were treated with helicid (purity >98%; Tokyo Chemical Industry Co., Ltd., Tokyo, Japan). After 24 h of incubation, 200 μg/mL of LPS was added to each well and the cells were incubated for an additional 24 h. Then, total RNA or protein of each group of cells was extracted for subsequent analysis. The specific groups were as follows: control, LPS, LPS + HEL, LPS + HEL + NC, and LPS + HEL + si-SH2D5. The SH2D5 siRNA (RiboBio, Guangzhou, China) sequences were siRNA-SH2D5-001: CCU CGU GCC UGG AGA ATT; siRNA-SH2D5-002: CUC ACC AGG UCU UCA GAA ATT; and siRNA-SH2D5-003: CAG CCU GGA GAG AUU AAU ATT. siRNA-SH2D5-003 was identified as the most efficient sequence and, thus, selected for quantitative real-time polymerase chain reaction (qRT-PCR) analysis with a real-time PCR detection system (Bio-Rad Laboratories, Hercules, CA, USA).

The following groups of cells were used to determine the effects of helicid on the methylation status of the SH2D5 gene: control, LPS, LPS + HEL, and LPS+5-AzaD. Assessment of various concentrations of helicid (1, 10, 100, and 200 μM) determined that the optimal concentration was 100 μM. The total acting time of helicid was 48 hours, and since 100 μM helicid best met the requirements of this experiment, this concentration was used for subsequent experiments. SH2D5 expression was detected by qRT-PCR.

2.2. Determination of Cell Viability.
Cell viability was determined using the 2,5-diphenyl-2H-tetrazolium bromide (MTT) assay (BestBio, Shanghai, China). Briefly, cells were seeded into 96-well plates (4×10^3 cells per well), cultured in a humidified incubator for 12 h, and then treated with helicid for 24, 48, and 72 h under a humidified atmosphere of 5% CO2/95% air at 37 ˚C. Afterward, the culture solution was discarded and replaced with 10 μL of MTT solution and 100 μL of fresh DMEM, and the plates were incubated for an additional 4 h. Then, 110 μL of formazan solution was used in place of that original medium and placed on a plate shaken at low speed for 10 min to allow adequate dissolution. The absorbance of each well was measured at 570 nm by a microplate reader (Bio-Rad Laboratories).

2.3. RNA Extraction and qRT-PCR Analysis.
For total RNA extraction, the culture medium was discarded and the cells were washed with phosphate-buffered saline (PBS; Thermo Fisher Scientific). Then, 1 mL of 0.25% trypsin (Beyotime Institute of Biotechnology) was added to each well to separate the cells from the bottom of the wells. Afterward, DMEM supplemented with fetal bovine serum was added to inactivate the trypsin and the cells were transferred to a RNase-free centrifuge tube and centrifuged at $300 \times g$ for 5 min. Then, the cell pellet was collected, mixed with 1 mL TRNzol Universal Reagent (Tiangen Biotech Co., Ltd., Beijing, China), and cultured at room temperature for 5 min to completely isolate the nucleic acid protein complex. Add 0.2 mL chloroform (Shanghai Richjoint Chemical Reagents Co., Ltd., Shanghai, China) to the mixture and shake quickly for 15 s, incubated at room temperature for 3 min and then centrifuged at 4°C and 12000 rpm (~$13400 \times g$) for 15 min. Then, the uppermost RNA-rich aqueous phase (500 μL) was transferred to a new centrifuge tube, mixed well with an equal volume of isopropanol (Shanghai Richjoint Chemical Reagents Co., Ltd.), and finally centrifuged at 4 ˚C and 12000 rpm (~$13400 \times g$) for 10 min. Then, a small amount of white precipitated RNA at the bottom of the tube was resuspended in 1 ml of precooled ethanol and centrifuged. Then, just leave the white sediment we need and suspend it in 20 μL of diethyl pyrocarbonate (DEPC)-treated water. For purpose of reverse to transcribe RNA into complementary DNA (cDNA), we use a High-Capacity cDNA Reverse Transcription Kit (Thermo Fisher Scientific). qRT-PCR was performed using a One-step RT-qPCR Kit (Tiangen Biotech Co., Ltd.) with the primers listed in Table 1, which were synthesized by RiboBio Co., Ltd. (Guangzhou, China). Relative gene expression levels were determined by the $2^{-\Delta\Delta Ct}$ method of glyceraldehyde 3-phosphate dehydrogenase (GAPDH) as an internal reference.

2.4. Protein Extraction and Western Blot Analysis.
Discard the medium of the six-well plate and wash the cells twice with PBS. Then, 100 μL of freshly prepared lysate (Beyotime Institute of Biotechnology, Haimen, China) was added to each hole of the six-well plate, and the plate was placed on ice cracking 10 min. Cells were then carefully scraped through each set of wells and transferred to labeled centrifuge tubes, which was centrifuged at 14000 rpms and 4°C for 10 min. After

TABLE 1: Primer sequences for qRT-PCR.

Name	Forward primer (5′-3′)	Reverse primer (5′-3′)
SH2D5	CACCAACTGGAGGGTTCGTAG	GCTGTTTGTACCATGCGATCA
Bax	CAAGAAGCTGAGCGAGTGTC	ATCCTCTGCAGCTCCATGTT
Bcl-2	GCATGCGACCTCTGTTTGAT	CAGGTATGCACCCAGAGTGA
Bad	GGACAGGCAGCCAATAACAG	TAAGCTCCTCCTCCATCCCT
Daxx	TCAATGGGCGTGTCTCTTCT	ATCTTCCACCCACTGTCCTG
CytC	AGACTATCCATGGAAGCAAG	GTTCCACTGTCTGTCTCAATA
Caspase9	CACGGCTTTGATGGAGATGG	TCTCTCGATGGACACAGAGC
Caspase3	AATTCAAGGGACGGGTCATG	TGACACAATACACGGGATCTG
GAPDH	GAACGGGAAGCTCACTGG	GCCTGCTTCACCACCTTCT

centrifugation, the supernatant of each cell group was removed and mixed with 5 × loading buffer (Beyotime Institute of Biotechnology) at a ratio of 1 : 4. Then, the EP tube was clamped to explosion-proof clamp and the proteins were denatured by boiling. The total concentration of protein in each group was determined by a bicinchoninic acid assay (Beyotime Institute of Biotechnology). Each group protein was separated using electrophoresis at 90 V for 100 min and then transferred to a nitrocellulose membrane at 110 V for 75 min. The membrane was blocked with skimmed milk for 2 h and then incubated with antibodies against SH2D5, Bax, Bad, Daxx, Bcl-2, caspase3, caspase9, and CytC (dilution, 1 : 1000; Cell Signaling Technology, Inc., Danvers, MA, USA) while shaking it all night on a 4°C shaker. Subsequently, we washed the membranes (three times for 15 min, each wash) with TBST and incubated them with goat anti-rabbit (1:3,000, Abcam, Cambridge, MA, USA) for 2 h at 26±2°C. Afterwards, the membranes were rinsed with TBST (three times/15 min each). We then visualized western blot bands using the ECL detection system (Bio-Rad).

2.5. Bisulfite Sequencing/PCR. MethPrimer online software (http://www.urogene.org/methprimer/) was used to obtain information of the CpG island of the SH2D5 gene promoter region and to design methylation-specific PCR (MSP) primers. The genomic DNA was extracted, treated with an EZ DNA Methylation-Direct Kit (Tiangen Biotech Co., Ltd.), and purified. Each MSP reaction consisted of 1 μL of vulcanized DNA as a template, 1 μL of upstream and downstream primers, 1.6 μL of dNTPs (2.5 nM), 0.4 μL of MSP DNA polymerase (2.5 U/μL), and 2.0 μL of 10× MSP PCR buffer, and finally add ddH2O to the volume to 20 μL. The reaction conditions were 94°C for 5 min, followed by 35 cycles at 94°C for 20 s, 60°C for 30 s, and 72°C for 20 s, with a final extension step at 72°C for 5 min. The obtained PCR product was placed in a gel electrophoresis apparatus filled with 2% gel into electrophoresis separation. The obtained electrophoretic bands were purified with a commercial agarose gel DNA recovery kit (Tiangen Biotech Co., Ltd.). The cells were transfected with the purified product with the pLB vector (Tiangen Biotech Co., Ltd.). Finally, the bacterial cells were cultured on LB solid medium containing ampicillin

(Beyotime Institute of Biotechnology) and then sequenced by Anhui General Biosystems, Inc. (Anhui, China).

2.6. Statistical Analysis. The Western blots were placed into ImageJ for analysis (https://imagej.nih.gov/ij/download.html). All data analyses were conducted using IBM SPSS Statistics for Windows, version 27.0 (IBM Corporation, Armonk, NY, USA). Plots were generated using Prism 7.0 software (GraphPad Software, Inc., San Diego, CA, USA). The data are presented as the mean ± standard deviation, as determined by one-way variance analysis with Tukey's test. A probability (p) value of <0.05 was considered statistically significant.

3. Results

3.1. Effects of LPS and Helicid on SH2D5 and C6 Cell Proliferation. As shown in Figure 2, the content of SH2D5 decreased at 24 h of LPS stimulation ($p < 0.001$) and there was no significant difference between 6 and 12 h, as shown in Figure 2(a). The addition of helicid at more than 100 μM to LPS-stimulated cells significantly increased ($p < 0.001$) SH2D5 expression, as shown in Figure 2(b). The results of the MTT assay showed that 100 μM helicid had no effect on the proliferation of C6 cells within 72 h, as shown in Figure 2(c).

3.2. Effect of SH2D5 on the CytC/Caspase9/Caspase3 Signaling Pathway. As shown in Figures 3 and 4, in order to determine the transfection efficiency of SH2D5 overexpression plasmid, we used qRT-PCR to detect the expression of SH2D5 in each group. SH2D5 was higher in the LPS+SH2D5 overexpression group than in the LPS + NC group ($p < 0.05$), while expression of the LPS group was lower than that in the control group ($p < 0.001$). There was no significant difference of SH2D5 expression between the LPS and LPS + NC groups, as shown in Figure 3(a). Then, the expression levels of Bax, Bcl-2, Bad, and Daxx were determined in LPS-induced C6 cells as a model of neuroinflammation. The experimental results showed the expression level of Bax, Bad, and Daxx was higher in the LPS group than the control group ($p < 0.001$ and <0.01, respectively), while the expression of Bcl-2 in the LPS group was higher than that in the control group ($p < 0.001$). As compared with the LPS + NC group, overexpression of
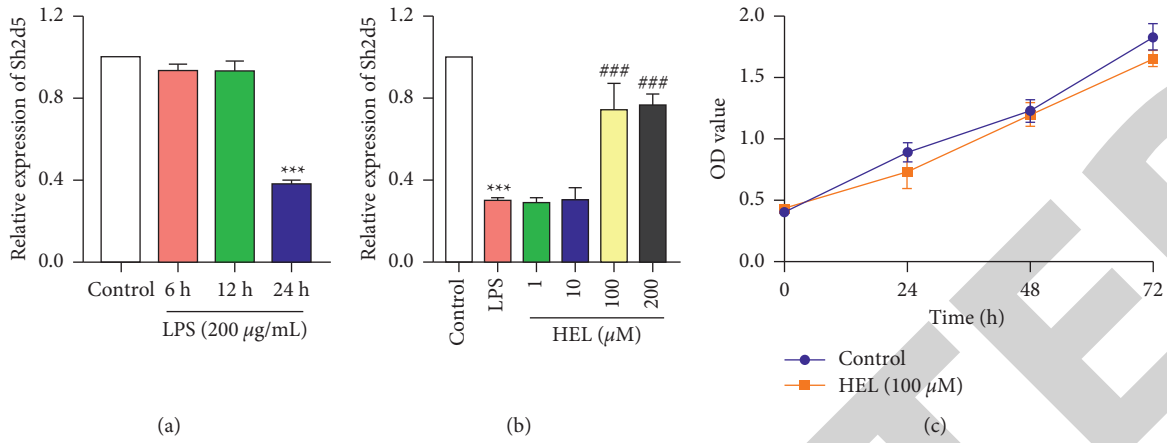
(a) (b) (c)

Figure 2: Effect of LPS or helicid on SH2D5 expression. (a) Effect of 200 μg/μL LPS on SH2D5 expression of different time periods. (b) Effects of different concentrations of helicid on SH2D5 expression. (c) Effects of helicid on the proliferation of C6 cells in different time periods. ***$p < 0.001$, control vs LPS; ###$p < 0.001$, LPS + HEL vs LPS. All data are expressed as the mean ± SEM.
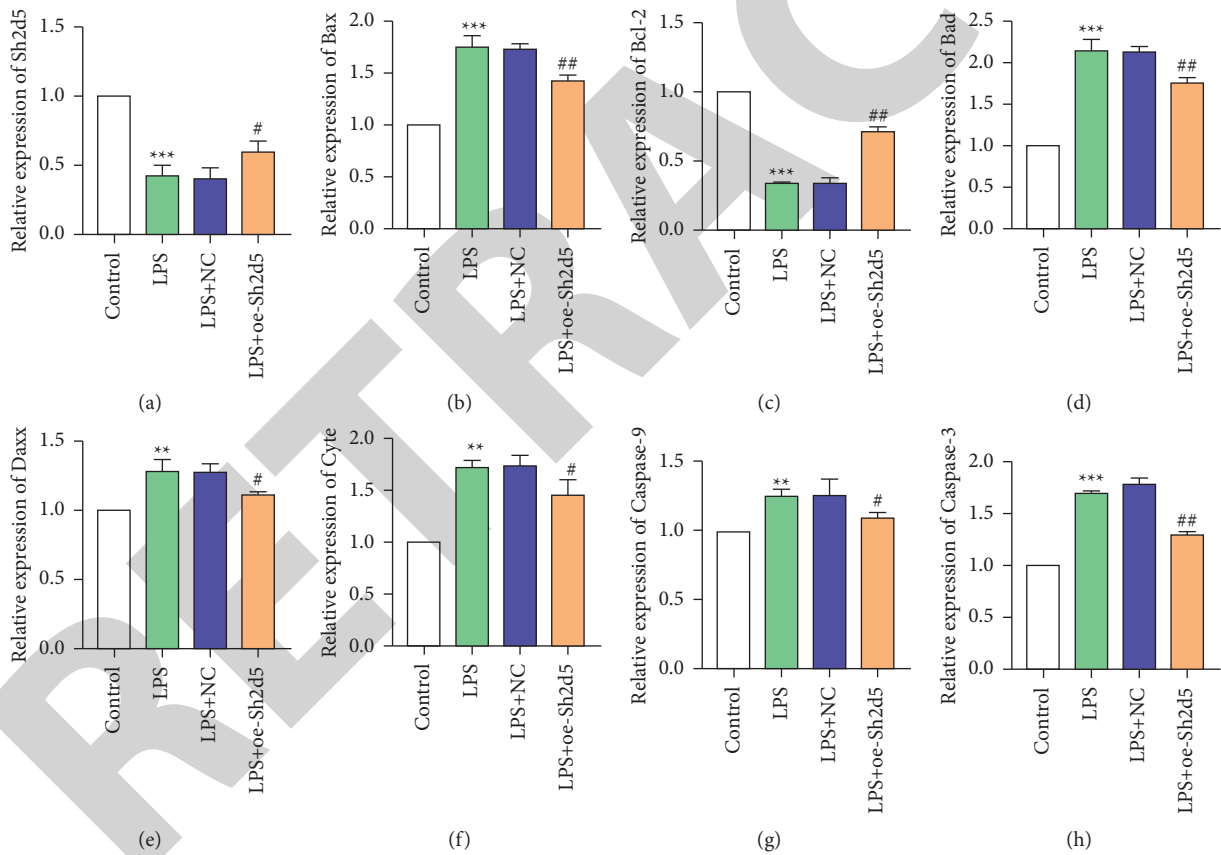

(a) (b) (c) (d)

(e) (f) (g) (h)

Figure 3: The changes of apoptotic functional indexes after overexpression of SH2D5 were detected by qRT-PCR. (a–h) The expression statistics of SH2D5, Bax, Bcl-2, Bad, Daxx, CytC, caspase9, and caspase3, respectively. **$p < 0.01$, ***$p < 0.001$, control vs LPS; #$p < 0.05$; ##$p < 0.01$, LPS + NC vs LPS + oe-SH2D5. All data are expressed as the mean ± SEM.

SH2D5 on the basis of LPS reduced the expression of Bax, Bad, and Daxx ($p < 0.01$ and <0.05, respectively), while the expression of Bcl-2 was higher in the LPS+SH2D5 over-expression group than the LPS + NC group ($p < 0.01$). There was no significant difference in the expression of any of the apoptosis markers between the LPS and LPS + NC groups, as

shown in Fig. 3(b-e). According to the transcriptome and postvalidation results, SH2D5 plays an important role in activation of the CytC/caspase9/caspase3 signaling pathway. Through qRT-PCR results, we could clearly see that the expression levels of CytC, caspase9, and caspase3 in the LPS group were increased relative to the control group ($p < 0.01$
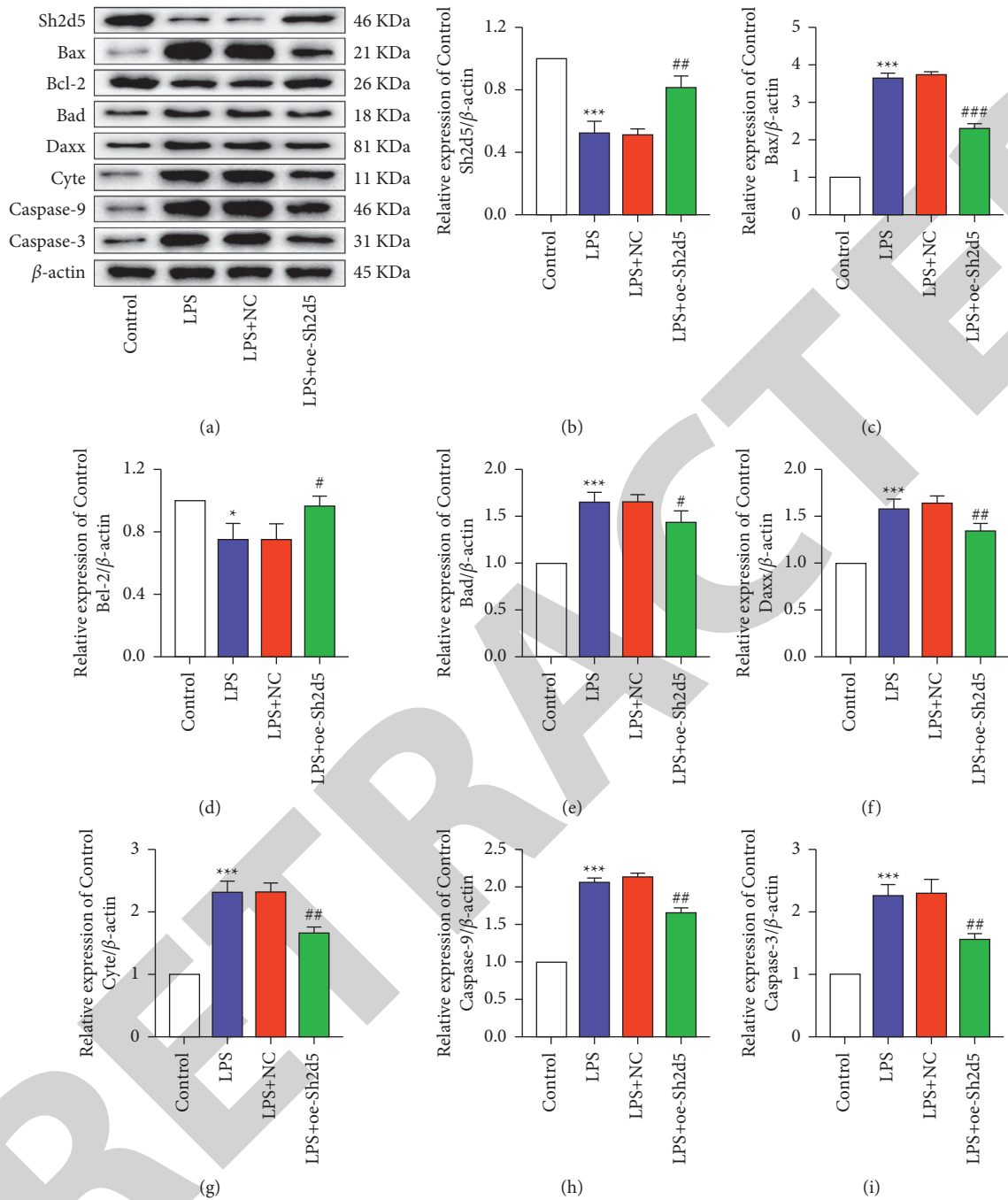
FIGURE 4: The changes of apoptotic functional indexes after overexpression of SH2D5 were detected by Western blot. (a) Protein bands. (b–i) The expression statistics of SH2D5, Bax, Bcl-2, Bad, Daxx, CytC, caspase9, and caspase3, respectively. * $p < 0.05$; *** $p < 0.001$, control vs LPS; $^{#}$ $p < 0.05$; $^{##}$ $p < 0.01$; $^{###}$ $p < 0.001$, LPS vs LPS + oe-SH2D5. All data are expressed as the mean ± SEM.

and <0.001, respectively). As compared with the LPS + NC group, after SH2D5 is overexpressed on the basis of LPS-induced, the expression levels of CytC, caspase9, and caspase3 were lower in the LPS+SH2D5 overexpression group than the LPS + NC group ($p < 0.05$ and <0.01, respectively), while there was no significant difference between the LPS and LPS + NC groups, as shown in Figures 3(f)–3(h). Western blot results were consistent with qRT-PCR results, as shown in Figures 4(a)–4(i).

3.3. Function of Helicid and Rescue Experiment. As shown in Figures 5 and 6, in order to explore the effects of helicid and silencing of SH2D5 on the apoptosis indices, three siRNA fragments were designed for silencing of SH2D5 in C6 cells. The qRT-PCR results showed that the three siRNA fragments all reduced SH2D5 mRNA levels in C6 cells ($p < 0.01$ and < 0.001, respectively). The siRNA-3 fragment had the best interference efficiency which was, therefore, used in the following experiment. There was no
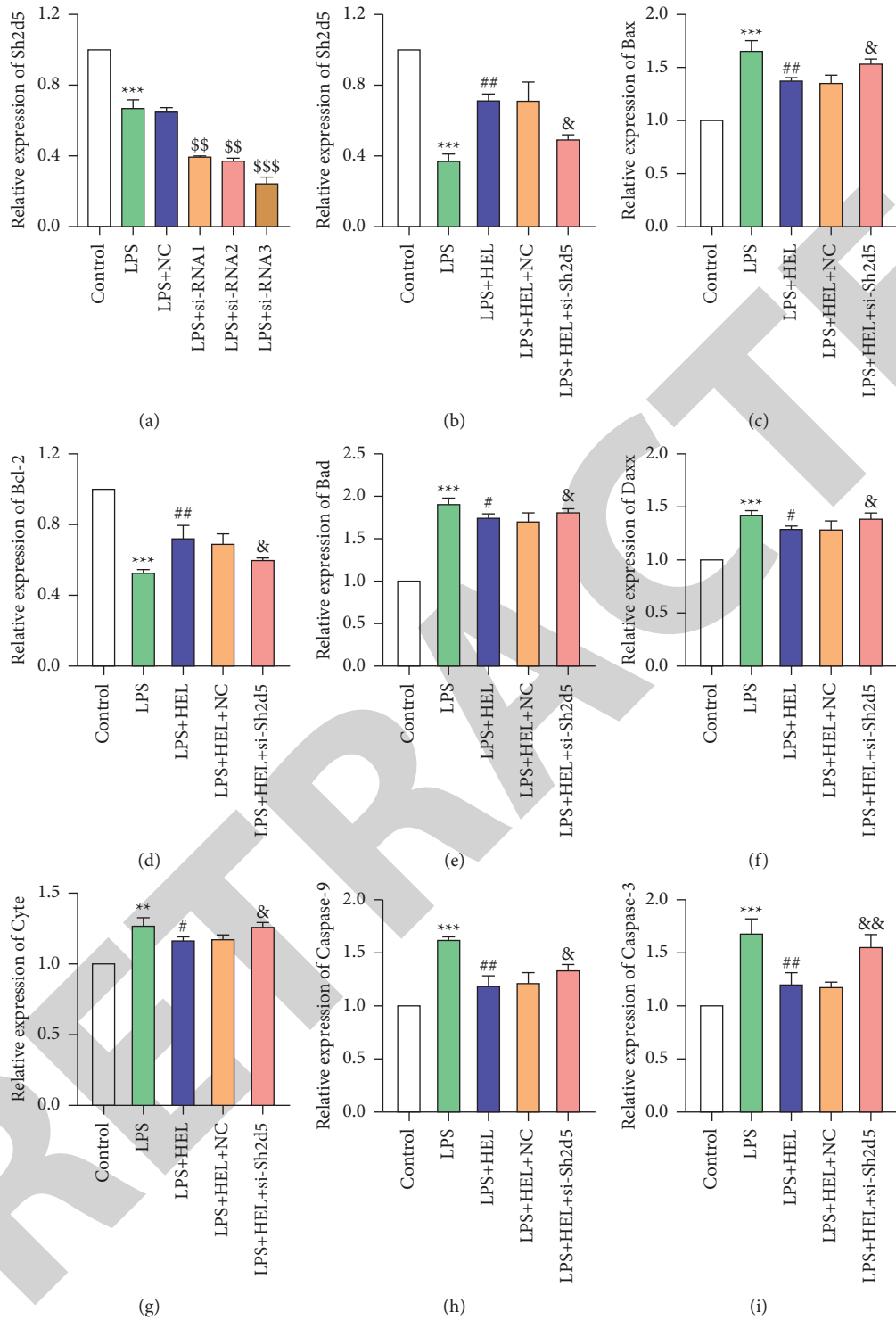
FIGURE 5: The effect of helicid on apoptosis index and the rescue experiment of SH2D5 were detected by qRT-PCR. (a) Efficiency detection of SH2D5 silenced fragments. (b) The expression of SH2D5 in each group was detected. (c–i) The expression statistics of Bax, Bcl-2, Bad, Daxx, CytC, caspase9, and caspase3, respectively. $^{**}p < 0.01$, $^{***}p < 0.001$, control vs LPS; $^{\$\$}p<0.01$; $^{\$\$\$}p<0.001$, LPS + NC vs LPS + siRNA; $^{\#}p<0.05$; $^{\#\#}p<0.01$, LPS vs LPS + HEL; $^{and}p<0.05$; $^{andand}p<0.01$, LPS + HEL + NC vs LPS + HEL + si-SH2D5. All data are expressed as the mean ± SEM.

significant difference in SH2D5 expression between the LPS and LPS + NC groups, as shown in Figure 5(a). The expression of SH2D5 in LPS group was lower than that in

control group ($p < 0.001$) and higher in the LPS + HEL group than the LPS group ($p < 0.01$). The addition of helicid and siRNA reduced the content of SH2D5 in the

(a)

(b)

(c)
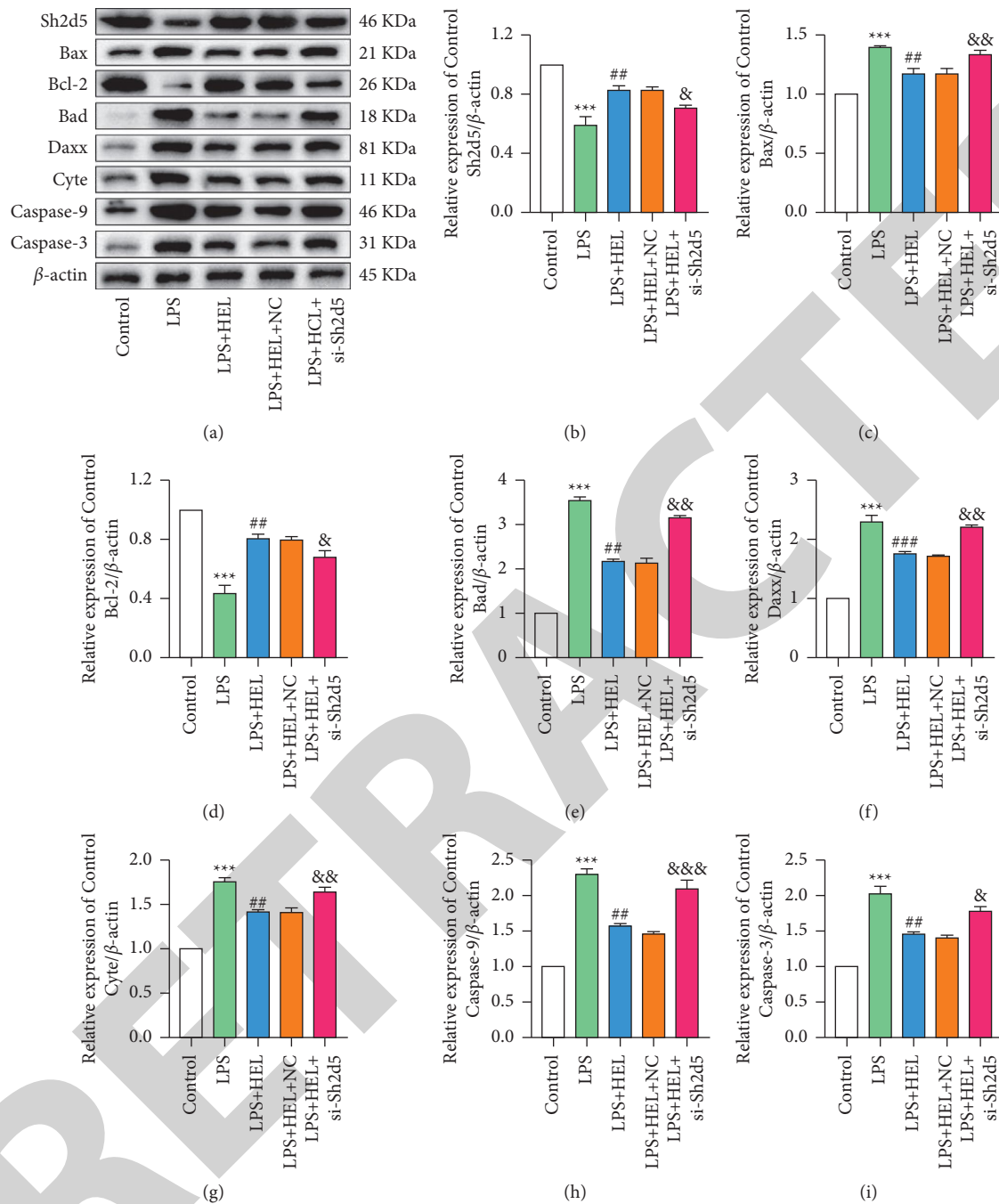
(d)

(e)

(f)

(g)

(h)

(i)

FIGURE 6: The effect of helicid on apoptosis and the rescue experiment of SH2D5 were detected by Western blot. (a) Protein bands. (b–i) The expression statistics of SH2D5, Bax, Bcl-2, Bad, Daxx, CytC, caspase9, and caspase3, respectively. ***$p < 0.001$, control vs LPS; ##$p<0.01$; ###$p<0.001$, LPS vs LPS + HEL; and $p<0.05$; andand $p<0.01$; andandand $p<0.001$, LPS + HEL + NC vs LPS + HEL + si-SH2D5. All data are expressed as the mean ± SEM.

LPS + HEL + si-SH2D5 group as compared to the LPS + HEL + NC group ($p < 0.05$). There was no significant difference in SH2D5 expression between the LPS + HEL + NC and LPS + HEL groups, as shown in Figure 5(b). The expression levels of Bax, Bad, and Daxx were lower in the LPS + HEL group than the LPS group ($p < 0.01$ and < 0.05, respectively), while the expression of Bcl-2 was higher in the LPS + HEL group than the LPS group ($p < 0.05$). The effect of helicid was partially reversed by silencing of SH2D5. As compared with the LPS + HEL + NC group, the expression levels of Bax, Bad, and Daxx were increased in the LPS + HEL + si-SH2D5 group (all, $p < 0.05$), while the expression of Bcl-2 in LPS + HEL + si-SH2D5 group was lower than that LPS + HEL + NC group ($p < 0.05$). There was no significant difference in the expression of each index between

(a)
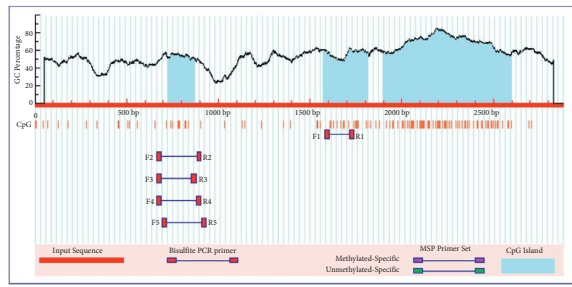
F: 5'-GGGCTGGCAAGATGGCTCTGCCAC-3'

GGGCTGGCAAGATGGCTCTGCCACTAAGAGCATTTGCTGCTCACC
CAGAGGACC**CG**GGGTTGTGTTCTTAGCACC**CG**TGTGGTAGCT**CG**A
AACCATCTGTAATTCTAGTTCTGGAAG**CGCG**ACCCCC**CG**CCTTCTG
TTCTGTGAGGAACCCAGGCA**CG**CA**CGCG**ATATACAAACA**CG**CAT
GCAGGCAAAACACTCATAAATCTGGGCAGAGAAATGC

F: 5'-ACATTTCTCTACCCAAATTTATAAATATTT-3'
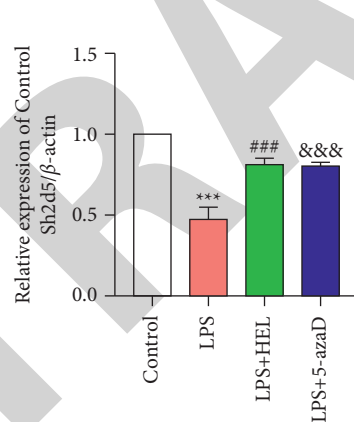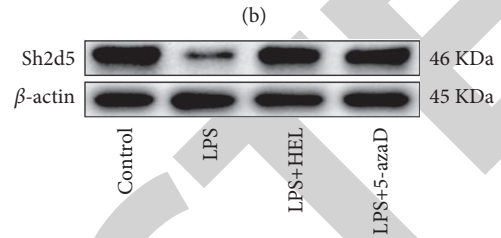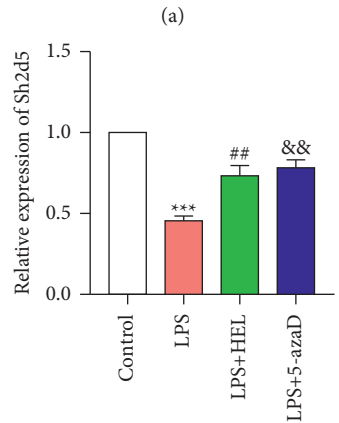
(b)

(d)

(c)

(e)

Figure 7: The MethPrimer online software predicts the CpG island in SH2D5 promoter region and the influence of helicid and 5-AzaD on SH2D5 expression. (a) It is predicted that the promoter region of SH2D5 gene contains CpG island. (b) BSP primers targeting CpG island in SH2D5 promoter region were designed by methyl primer software, and CpG dinucleotide was highlighted. (c) The expression of SH2D5 was detected by qRT-PCR. (d) Protein bands. (e) Statistical diagram of SH2D5 protein expression. $^{***}p<0.001$, control vs LPS; $^{##}p<0.01$; $^{###}p<0.001$, LPS vs LPS + HEL; $^{andand}p<0.01$; $^{andandand}p<0.001$, LPS vs LPS+5-AzaD. All data are expressed as the mean ± SEM.

the LPS + HEL + NC and LPS + HEL groups, as shown in Figures 5(c)–5(f). In order to determine whether helicid affects the CytC/caspase9/caspase3 signaling pathway by regulating the expression of SH2D5, SH2D5 was silenced by the addition of helicid. The expression levels of CytC, caspase9, and caspase3 were lower in the LPS + HEL group than the LPS group ($p < 0.05$ and <0.01, respectively) and higher in the LPS + HEL + si-SH2D5 group than the LPS + HEL + NC group ($p < 0.05$ and <0.01, respectively), while there was no significant difference

between the LPS + HEL + NC and LPS + HEL groups, as shown in Figures 5(g)–5(i). The Western blot experiment again verified that the results were consisting in those of qRT-PCR, as shown in Figures 6(a)–6(i).

3.4. DNA Methylation Level of the SH2D5 Promoter. As shown in Figures 7 and 8, the 2000 BP sequence upstream of the SH2D5 transcription initiation site is generally considered as the promoter of SH2D5. In order to find the
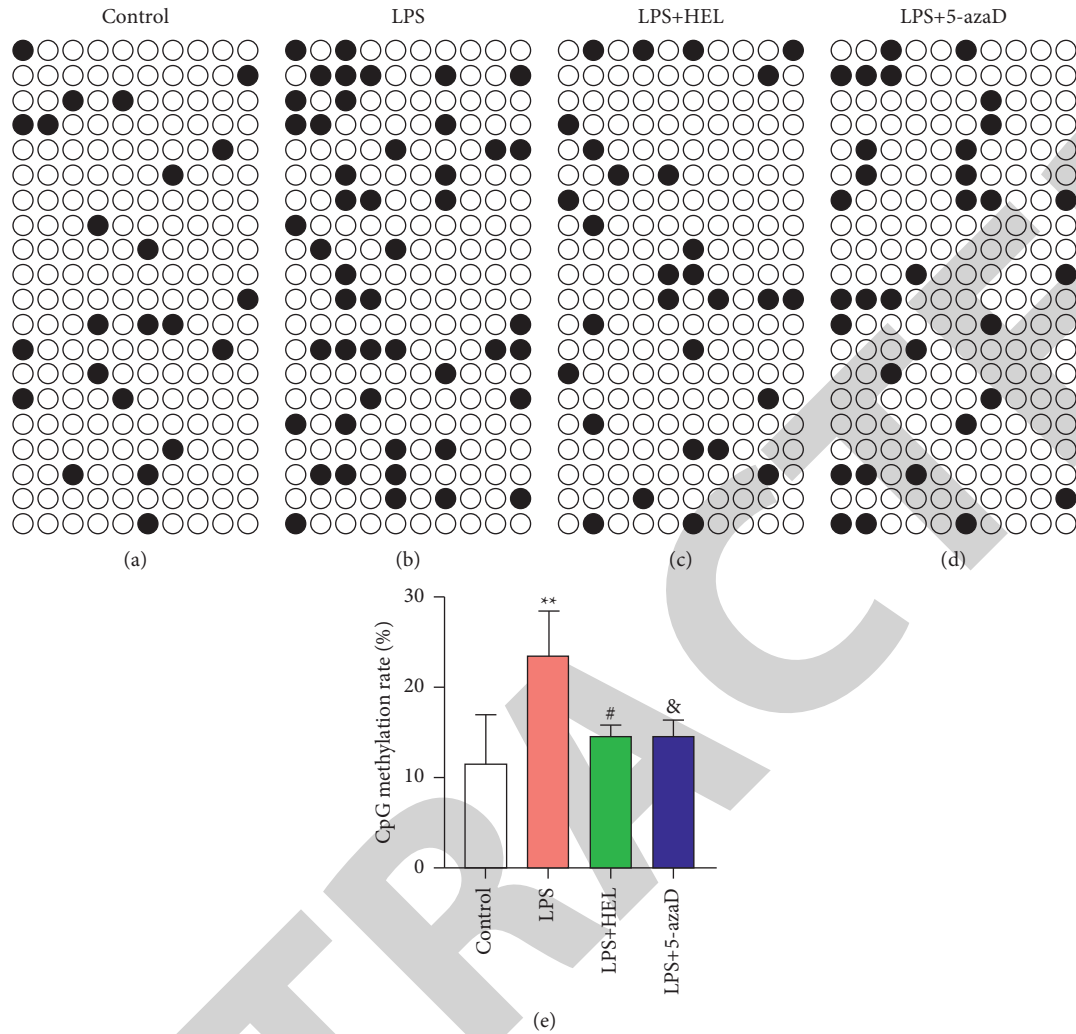
Figure 8: Effect of helicid or 5-AzaD on DNA methylation in SH2D5 promoter region. (a–d) The SH2D5 DNA methylation levels of each group. (e) Statistical chart of DNA methylation rates of each group. $^{**}p<0.01$, control vs LPS; $^{#}p<0.05$, LPS vs LPS + HEL; $^{and}p<0.05$, LPS vs LPS+5-AzaD. All data are expressed as the mean ± SEM.

CpG island of SH2D5 promoter, we use MethPrimer online software to predict. We found three CpG islands in the promoter region of SH2D5, as shown in Figure 7(a). The designed primers targeting the CpG island in the promoter region of SH2D5 revealed 10 CpG loci located in the promoter region of SH2D5, with an abundance of CG dinucleotides, as shown in Figure 7(b). Also, the relative expression of SH2D5 was detected in each group by qRT-PCR and Western blot analyses. As compared with the LPS group, the expression of SH2D5 in LPS + HEL group ($p < 0.01$) and LPS+5-AzaD ($p < 0.01$) group increased, while there was no significant difference between the LPS + HEL and LPS+5-AzaD groups, as shown in Figures 7(c)–7(e). The DNA methylation rate of SH2D5 promoter region in control group was lower than that in LPS group ($p < 0.01$). Notably, the DNA methylation rate of the SH2D5 promoter region was lower in the LPS + HEL group than the LPS group ($p < 0.05$). The methylation rate of the SH2D5 promoter region was also lower in the

LPS+5-AzaD group than the LPS group ($p < 0.05$), while there was no significant difference between the LPS + HEL and LPS+5-AzaD groups, as shown in Figures 8(a)–8(e).

4. Discussion

In this study, overexpression of SH2D5 and treatment with helicid increased the expression levels of the proapoptotic indices in C6 cells stimulated by LPS and inhibited activation of the CytC/caspase9/caspase3 signaling pathway, while silencing of SH2D5 by the addition of helicid reversed these effects. Treatment with helicid and 5-AzaD decreased the DNA methylation rate of the CpG island of the SH2D5 promoter region.

C6 cells are clones of rat glioma cells that are widely used in pathological research and screening of drugs for treatment of nervous system diseases, especially neuro-inflammatory diseases [27]. LPS, also known as endotoxin, is often used to induce inflammation and apoptosis in the

experiment and is the main component of the cell wall of Gram-negative bacteria. In this study, C6 glial cells were used as an in vitro model [28]. The results showed that LPS-stimulated C6 cells to produce an inflammatory response. The LPS-induced C6 cell neuritis model is considered a classic model of inflammation. Therefore, LPS-stimulated C6 cells were used as an in vitro model of depression [29].

Apoptosis is the main form of cell death in many neurological diseases, including depression, Alzheimer's disease, Parkinson's disease, Huntington's disease, stroke, and amyotrophic lateral sclerosis [30]. The main molecular components of neuronal apoptosis include Bcl-2, Bax, and caspase family proteins. Previous studies have reported that increased expression of cleaved caspase3 is a marker of apoptosis in neurological diseases. Overexpression of Bax promotes cell apoptosis, while the heterodimer formed into Bax and Bcl-2 homologues (Bcl-2 and Bcl-xl) with the function of death inhibition inhibited the cell death promoting effect of Bax. The sensitivity of cells to apoptosis stimulation is regulated by the relative expression of different Bcl-2 family proteins [31]. Therefore, the expression levels of cleaved caspase-3 and Bax are significantly increased during cell apoptosis, while expression of Bcl-2 is significantly decreased. In the process of LPS-induced damage to the electron transport chain, mitochondria can experience a "permeability transition" state induced by reactive oxygen species/active nitrogen species, which is highly related to the rapid increase in mitochondrial inner membrane permeability [32]. Transient permeability can result in mitochondrial swelling, giving rise to rupture of the mitochondrial outer membrane and the release of cytochrome C, which triggers caspase activation. In the present study, overexpression of SH2D5 or treatment with helicid reversed the increased expression levels of Bax, CytC, and cleavage caspase3 and decreased Bcl-2 levels, indicating that SH2D5 or helicid has a strong antiapoptotic effect on central nervous system cell lines [33, 34].

DNA methylation is one of the most heritable epigenetic modifications that affect gene expression without changing DNA sequence. The modulation of DNA methylation is deemed to be related to gene expression control [35]. The popular view is that hypermethylation leads to transcriptional inhibition. DNA methylation is particularly interesting in the context of neuropsychiatric diseases [36]. Environmental factors that usually affect disease trajectory can change the methylation pattern. Recent evidence shows that changes in DNA methylation (i.e., hypermethylation and hypomethylation at the same site) and methylation variation often exist in individuals with depression. So far, most knowledge about the epigenetic mechanism of depression has been obtained from animal research and more recently confirmed in human studies. Genome-wide DNA methylation analysis of patients with depression for the first time found significant differences in DNA methylation of genes related to neuronal growth and development [37]. It has been confirmed that BDNF is involved in depression-related behavioral phenomena and the therapeutic effect of antidepressants. The higher degree of CpG methylation of the BDNF promoter region is associated with a significant

decrease in the synthesis of this factor in neurons [38]. In addition, it has been confirmed that the methylation levels of the BDNF promoter are elevated in patients with depressive symptoms and those with suicidal ideation. Interestingly, decreased BDNF methylation was observed in response to treatment with antidepressants [39, 40]. Therefore, DNA methylation is a potential biomarker to predict depression and the response to antidepressants. Further evidence suggests that antidepressants play a role, at least in part, through epigenetic modification, and the epigenetic changes observed in patients with depression can be used as a predictor of the response to antidepressants [41]. Antidepressants may also have the ability to change or even reverse epigenetic modifications, suggesting that the therapeutic response may be indicated by the methylation status of some genes [42]. In this experiment, helicid improved the apoptosis index by regulating DNA methylation of the SH2D5 promoter and regulating the CytC/caspase9/caspase3 signaling pathway.

5. Conclusion

The antidepressant effect of helicid involves regulation of the CytC/caspase9/caspase3 signaling pathway by mediating SH2D5 DNA methylation and can improve LPS-induced apoptosis of C6 cells. These experimental results provide insights into the potential therapeutic value of helicid or SH2D5 in the treatment of depression, although further studies are needed to elucidate the exact mechanism of the antidepressant-like effects.

Data Availability

The simulation experiment data used to support the findings of this study are available from the corresponding author upon request.

Disclosure

Yuan Zhang and Mei Wang are the joint first authors of this work.

Conflicts of Interest

The authors declare that there are no conflicts of interest regarding the publication of this study.

Acknowledgments

References

[1] X. Guo, P. Wu, and X. Cui, "Pre- and post-treatment levels of plasma metabolites in patients with bipolar depression," *Frontiers in Psychiatry*, vol. 12, Article ID 747595, 2021.

[2] E. Dale, B. Bang-Andersen, and C. Sánchez, "Emerging mechanisms and treatments for depression beyond SSRIs and SNRIs," *Biochemical Pharmacology*, vol. 95, no. 2, pp. 81–97, 2015.

[3] M. Ruggeri, C. Drago, D. Mandolini, P. Francesa Morel, C. Mencacci, and F. Starace, "The costs of treatment resistant depression: evidence from a survey among Italian patients," *Expert Review of Pharmacoeconomics & Outcomes Research*, vol. 26, pp. 1–8, 2021.

[4] Y. Dai, T. Wei, Z. Shen, Y. Bei, H. Lin, and H. Dai, "Classical HDACs in the Regulation of Neuroinflammation," *Neurochemistry International*, vol. 150, Article ID 105182, 2021.

[5] Y. Chen, L. Li, J. Zhang et al., "Dexmedetomidine Alleviates Lipopolysaccharide-Induced Hippocampal Neuronal Apoptosis via Inhibiting the P38 MAPK/c-Myc/CLIC4 Signaling Pathway in Rats," *Molecular neurobiology*, vol. 58, no. 11, pp. 5533–5547, 2021.

[6] I. Marinescu, D. Marinescu, L. Mogoantă, I. C. Efrem, and P. O. Stovicek, "SARS-CoV-2 infection in patients with serious mental illness and possible benefits of prophylaxis with Memantine and Amantadine," *Rom J Morphol Embryol*, vol. 61, no. 4, pp. 1007–1022, 2020.

[7] L. A. R. Cyrino, D. Delwing-de Lima, O. M. Ullmann, and T. P. Maia, "Concepts of neuroinflammation and their relationship with impaired mitochondrial functions in bipolar disorder," *Frontiers in Behavioral Neuroscience*, vol. 15, Article ID 609487, 2021.

[8] Z. Zhao and A. Fu, "Mitochondrial therapy: a new strategy for treating mitochondrion-associated diseases," *Chinese Journal of Biotechnology*, vol. 37, no. 4, pp. 1168–1177, 2021.

[9] W. Zhang, F. Zhang, Q. Hu et al., "The emerging possibility of the use of geniposide in the treatment of cerebral diseases: a review," *Chinese Medicine*, vol. 16, no. 1, p. 86, 2021.

[10] Y. Liu, Z. Cui, A. Yang et al., "Anti-apoptotic and pro-survival effect of exercise training on early aged hypertensive rat cerebral cortex," *Aging (Albany NY)*, vol. 13, 2021.

[11] A. Djordjevic, J. Djordjevic, I. Elaković, M. Adzic, G. Matić, and M. B. Radojcic, "Fluoxetine affects hippocampal plasticity, apoptosis and depressive-like behavior of chronically isolated rats," *Progress in Neuro-Psychopharmacology and Biological Psychiatry*, vol. 36, no. 1, pp. 92–100, 2012.

[12] M. S. Simon, C. Schiweck, G. Arteaga-Henríquez et al., "Monocyte mitochondrial dysfunction, inflammaging, and inflammatory pyroptosis in major depression," *Progress in Neuro-Psychopharmacology and Biological Psychiatry*, vol. 111, Article ID 110391, 2021.

[13] D. Glavan, V. Gheorman, A. Gresita, D. M. Hermann, I. Udristoiu, and A. Popa-Wagner, "Identification of transcriptome alterations in the prefrontal cortex, hippocampus, amygdala and hippocampus of suicide victims," *Scientific Reports*, vol. 11, no. 1, Article ID 18853, 2021.

[14] A. Kawatake-Kuno, T. Murai, and S. Uchida, "The molecular basis of depression: implications of sex-related differences in epigenetic regulation," *Frontiers in Molecular Neuroscience*, vol. 14, Article ID 708004, 2021.

[15] L. Li, T. Wang, S. Chen, Y. Yue, Z. Xu, and Y. Yuan, "DNA methylations of brain-derived neurotrophic factor exon VI are associated with major depressive disorder and antidepressant-induced remission in females," *Journal of Affective Disorders*, vol. 295, pp. 101–107, 2021.

[16] H.-H. Shi, H.-E. Liu, and X.-J. Luo, "Hypermethylation-mediated silencing of NDRG4 promotes pancreatic ductal adenocarcinoma by regulating mitochondrial function," *BMB Reports*, vol. 53, no. 12, pp. 658–663, 2020.

[17] A. Martinez-Pinteño, N. Rodriguez, A. Blázquez et al., "DNA methylation of fluoxetine response in child and adolescence: preliminary results," *Pharmgenomics Pers Med*, vol. 14, pp. 459–467, 2021.

[18] G. Kronenberg, M. Colla, and M. Endres, "Folic acid, neurodegenerative and neuropsychiatric disease," *Current Molecular Medicine*, vol. 9, no. 3, pp. 315–323, 2009.

[19] E. J. Gray, E. Petsalaki, D. A. James et al., "Src homology 2 domain containing protein 5 (SH2D5) binds the breakpoint cluster region protein, BCR, and regulates levels of Rac1-GTP," *Journal of Biological Chemistry*, vol. 289, no. 51, Article ID 35397, 2014.

[20] Y. Zheng, P. Ming, C. Zhu et al., "Hepatitis B virus X protein-induced SH2 domain-containing 5 (SH2D5) expression promotes hepatoma cell growth via an SH2D5-transketolase interaction," *Journal of Biological Chemistry*, vol. 294, no. 13, pp. 4815–4827, 2019.

[21] B. S. Winsvold, P. Palta, E. Eising et al., "Epigenetic DNA methylation changes associated with headache chronification: a retrospective case-control study," *Cephalalgia*, vol. 38, no. 2, pp. 312–322, 2018.

[22] J. Tong, Z. Zhou, W. Qi et al., "Antidepressant effect of helicid in chronic unpredictable mild stress model in rats," *International Immunopharmacology*, vol. 67, pp. 13–21, 2019.

[23] X.-Y. Li, W.-W. Qi, Y.-X. Zhang et al., "Helicid ameliorates learning and cognitive ability and activities cAMP/PKA/CREB signaling in chronic unpredictable mild stress rats," *Biological and Pharmaceutical Bulletin*, vol. 42, no. 7, pp. 1146–1154, 2019.

[24] Y. Zhang, D. Luan, Y. Liu et al., "Helicid reverses lipopolysaccharide-induced inflammation and promotes GDNF levels in C6 glioma cells through modulation of prepronociceptin," *Chemistry and Biodiversity*, vol. 17, no. 7, 2020.

[25] Y.-X. Zhang, X.-T. Zhang, H.-J. Li et al., "Antidepressant-like effects of helicid on a chronic unpredictable mild stress-induced depression rat model: inhibiting the IKK/IκBα/NF-κB pathway through NCALD to reduce inflammation," *International Immunopharmacology*, vol. 93, Article ID 107165, 2021.

[26] S. Vaidya, P. A. Shantanu, and V. Tiwari, "Attenuation of ongoing neuropathic pain by peripheral acting opioid involves activation of central dopaminergic neurocircuitry," *Neuroscience Letters*, vol. 754, Article ID 135751, 2021.

[27] H.-T. Zhang, M. Tian, Q.-W. He, N. Chi, C.-M. Xiu, and Y.-B. Wang, "Effect of Aster tataricus on production of inflammatory mediators in LPS stimulated rat astrocytoma cell line (C6) and THP-1 cells," *Saudi Pharmaceutical Journal*, vol. 25, no. 3, pp. 370–375, 2017.

[28] F.-W. Tseng, D.-Y. Liou, M.-J. Tsai, W.-C. Huang, and H. Cheng, "Cytoprotective and anti-inflammatory effects of PAL31 overexpression in glial cells," *Journal of Biomedical Science*, vol. 21, no. 1, p. 60, 2014.

[29] F. Fattahi, J. J. Grailer, M. Parlett et al., "Requirement of complement C6 for intact innate immune responses in mice," *The Journal of Immunology*, vol. 205, no. 1, pp. 251–260, 2020.

[30] M. Maes, M. Kubera, E. Obuchowiczwa, L. Goehler, and J. Brzeszcz, "Depression's multiple comorbidities explained by (neuro)inflammatory and oxidative & nitrosative stress pathways," *Neuroendocrinology Letters*, vol. 32, no. 1, pp. 7–24, 2011.

[31] J. Bas, T. Nguyen, and G. Gillet, "Involvement of bcl-xL in neuronal function and development," vol. 22, no. 6, 2021.

[32] C. Wang, Y. Li, Y. Li et al., "FAM134B-Mediated ER-phagy in Mg2+-free solution-induced mitochondrial calcium

homeostasis and cell death in epileptic hippocampal neurons," *Neurochemical Research*, vol. 46, no. 9, pp. 2485–2494, 2021.

[33] B. Yousefsani, S. Mehri, J. Pourahmad, and H. Hosseinzadeh, "Protective effect of crocin against mitochondrial damage and memory deficit induced by beta-amyloid in the Hippocampus of rats," *Iran J Pharm Res*, vol. 20, no. 2, pp. 79–94, 2021.

[34] X. Zhou, H. Chen, L. Wang et al., "Mitochondrial dynamics: a potential therapeutic target for ischemic stroke," *Frontiers in Aging Neuroscience*, vol. 13, Article ID 721428, 2021.

[35] B. Török, C. Fazekas, A. Szabó, and D. Zelena, "Epigenetic modulation of vasopressin expression in health and disease," *Int J Mol Sci*, vol. 22, no. 17, 2021.

[36] Z. Shirvani-Farsani, Z. Maloum, Z. Bagheri-Hosseinabadi, N. Vilor-Tejedor, and I. Sadeghi, "DNA methylation signature as a biomarker of major neuropsychiatric disorders," *Journal of Psychiatric Research*, vol. 141, pp. 34–49, 2021.

[37] F. Güiza, I. Vanhorebeek, S. Verstraete et al., "Effect of early parenteral nutrition during paediatric critical illness on DNA methylation as a potential mediator of impaired neurocognitive development: a pre-planned secondary analysis of the PEPaNIC international randomised controlled trial," *The Lancet Respiratory Medicine*, vol. 8, no. 3, pp. 288–303, 2020.

[38] A. E. Richter, I. Bekkering-Bauer, R. N. Verkaik-Schakel et al., "Altered neurodevelopmental DNA methylation status after fetal growth restriction with brain-sparing," *Journal of Developmental Origins of Health and Disease*, vol. 30, pp. 1–12, 2021.

[39] R. N. Mustafin, A. V. Kazantseva, R. F. Enikeeva, S. B. Malykh, and E. K. Khusnutdinova, "Longitudinal genetic studies of cognitive characteristics," *Vavilov Journal of Genetics and Breeding*, vol. 24, no. 1, pp. 87–95, 2020.

[40] J. Zhou, M. Li, X. Wang et al., "Drug response-related DNA methylation changes in schizophrenia, bipolar disorder, and major depressive disorder," *Frontiers in Neuroscience*, vol. 15, Article ID 674273, 2021.

[41] P. Wang, C. Zhang, Q. Lv et al., "Association of DNA methylation in BDNF with escitalopram treatment response in depressed Chinese Han patients," *European Journal of Clinical Pharmacology*, vol. 74, no. 8, pp. 1011–1020, 2018.

[42] P. Wang, Q. Lv, Y. Mao et al., "HTR1A/1B DNA methylation may predict escitalopram treatment response in depressed Chinese Han patients," *Journal of Affective Disorders*, vol. 228, pp. 222–228, 2018.